

Article ID: 1006-8775(2003) 01-0086-09

NUMERICAL SIMULATIONS OF β -GYRES IN TROPICAL CYCLONES

YANG Hong-bo (杨洪波), ZHANG Ming (张 铭)

(Meteorological Institute, China PLA University of Science & Technology, Nanjing, 211101 China)

ABSTRACT: The circulation of β -gyres in tropical cyclones is studied using numerical simulations. As shown in the result, there is clear circulation of β -gyres in the deviation flow field of the middle layer of the model, i.e. there is cyclone current west of the vortex center but anticyclone current east of it. The theory analysis shows that the circulation of β -gyres is formed by the advection of geostrophic vorticity.

Key words: tropical cyclones; β -gyres; numerical simulations

CLC number: P457.8 **Document code:** A

1 INTRODUCTION

Ever since the 1940's, the tropical cyclone (TC) has been viewed as a point vortex or rigid vortex. The prediction is summed up as one for airflow in the ambient field. The method usually succeeds. The steering theory for the airflow becomes its theoretical foundation. Though with some success, the actual track of TC movement can be much deviated from the steering current, as seen in routine forecast practice. Without much changes in the ambient steering current, the TC can have unexpected changes in the direction, speed of motion or intensity. A typical example would be for a TC vortex, locating in steady easterly airflow south of the western Pacific high, to make occasional passage through the ridge in an actual track that is almost normal to the steering current. It suffices to show that the theory does not account for all possibilities. It prompts one to look for factors responsible for the motion of the TC other than the ambient field flow. Over the period after it, the influence of β -effect on the movement and structure of TCs has aroused much interest. Holland^[1] states that the β -effect governs the motion of TCs in addition to the steering of ambient flow. The influence of β -effect on TC motion has become an attractive topic since mid-1980's.

For the study of the influence of β -effect on TC motion, Fiorino et al.^[2] decompose the stream function of the TC into axisymmetric and non-axisymmetric components to find that the β -effect can generate asymmetric circulation systems, i.e. β -gyres that are of reversed circulation in the east and west of the vortex and the ventilation flow between the asymmetric β -gyres represents the direction and velocity of the vortex motion. Being subjected to the β term, the TC circulation transforms from an initially axisymmetric field to a non-axisymmetric one. A deviation flow field is derived by subtracting the asymmetric field from the non-axisymmetric one. It is its characteristic that a quasi-homogeneous flow is found between a pair of vortexes in the deviation flow field. The direction and velocity of the flow are good indicators of those of TC center in the time to come.

Received date: 2001-03-05; **revised date:** 2003-01-10

Foundation item: National Science Foundation of China (49875008)

Biography: YANG Hong-bo (1972 -), male, native from Hubei Province, lab experimenter, M.S., mainly undertaking the study of fluid dynamics.

In their detailed analysis of the effects of non-linear advection of relative vorticity on TC structure and motion, Chen et al.^[3] clearly show that the non-linear advection and $\dot{\sigma}$ term are the kinds of intrinsic factors that affect the motion of TC. More recently, Chen and Xu et al.^[4,5] use in situ TC data from the SPECTRUM experiment to study the asymmetric deviation flow field of Tropical Cyclone Flo and its effect on thermally unstable asymmetric structure in the outer sector. They find that real TCs are with what Fiorino thought an asymmetric dipole system. It is proved at the same time that the effect of asymmetric structure of TC motion is not only reflected in the dynamic structure but the asymmetric thermodynamics. The latter causes apparent changes in TC motion, too. For further study of the influence of the $\dot{\sigma}$ -effect on the structure and motion track, the work has conducted a numerical experiment.

2 BRIEF ACCOUNT OF THE MODEL

For detailed description of the model, see [6]. Only a brief introduction is presented here. In the model, the governing equation is a baroclinic primitive equation in map-projected \mathbf{S} -coordinates. Horizontal isolines of latitude and longitude are used in the grid at the interval of Δq . All model physical quantities are assigned to the same horizontal grid point. In the vertical direction, layers are divided by equal \mathbf{S} intervals and difference grid intervals are adjustable at h , Δq and h . For the present run, the model takes horizontal grids by 61×61 with $\Delta q = 0.3^\circ$ and 10 vertical layers with $h=0.1$, which are numbered downward with k . Geopotential Φ and $\dot{\sigma}$ are defined to be within two layers of integral number while the remaining variables are defined on the layers with k being the integral number. Second-order centered difference is applied as spatial difference and forward difference iteration scheme is used in temporal difference. The model is of fixed lateral boundary. To decrease the effect of lateral boundary on waving, relaxation is added to the five circles close to the lateral boundary. The relaxation coefficient is decreasing inward from the boundary with non-linear transition. Additionally, values of the horizontal dissipation coefficient added to these circles to minimize adverse effects from the lateral boundary. Besides, the five circles near the lateral boundary are eliminated from the model output so that actual grids are distributed by 61×61 . For the sake of simplicity, the lower lateral boundary takes into account nothing but most simplified physics for the whole boundary layer, which includes the drag, sensible heat and evaporation. The upper boundary takes $\partial F / \partial \mathbf{S} = 0$ where F indicates the physical quantity in the model. The difference for the model pressure gradient is in of the Corpy format, which is useful for high terrain. The model does not include any terrain as the current deals specifically with tropical cyclones.

The model does not involve itself with any processes of radiation. There are two schemes for diabatic heating. The first does not include specific humidity in the model and the diabatic heating is realized by parameterizing the vertical motion at the top of the boundary layer. In other words, assuming that

$$Q_{i,j} = 10^3 \mathbf{d} \cdot G(k) \cdot w_{i,j} \quad (1)$$

where $w_{i,j}$ is the vertical velocity of the \mathbf{S} -coordinates at the top of the boundary layer (the 9th layer is taken), i.e. $\dot{\sigma}$; \mathbf{d} is an adjustable parameter so that heating feedback can be adjusted between 5.5 and 6.5, reflecting indirectly the magnitude of specific humidity field. When $\mathbf{d} = 0$, the diabatic heating term is absent. $G(k)$ is the function of vertical distribution of diabatic heating that expresses as

$$G(k) = \sin\left(\frac{k\mathbf{p}}{10}\right) + \frac{1}{2}\sin\left(\frac{2k\mathbf{p}}{10}\right) + \frac{1}{4}\sin\left(\frac{3k\mathbf{p}}{10}\right) \quad (2)$$

The scheme is called Scheme A in the work, which features simple and fast model runs in addition to quantitative modeling of the structure and motion of TC. It is too simplified to simulate precipitation, but it is still feasible for numerical study rather than routine forecast. The other attempt is to incorporate specific humidity in the model to give realistic simulation of the precipitation in TC. The scheme contains a diabatic process that employs large-scale condensation and improved Kuo's parameterization technique for cumulus convection. It is called Scheme B. It is complicated and consumes much computer time.

Taking the ideal field as initial field, the model takes assumptions as follows:

Temperature, geopotential height and surface pressure fields are set horizontally homogeneous and of their own typical values. A vertically consistent symmetric circular vortex is placed at the center of the integration domain of the initial wind field. The radial wind speed is zero and the tangential wind speed is given by

$$V = V_{\max} \frac{r}{r_{\max}} \cdot \exp\left(1 - \frac{r}{r_{\max}}\right) \quad (3)$$

in which r is the distance from any gridpoint of a layer to the vortex center, r_{\max} is the distance from the circle of the layer's maximum wind speed to the vortex center and V_{\max} is the maximum tangential wind speed on the maximum wind speed circle. From Eq.(3) we have $V = 0$ when $r = 0$; $V = V_{\max}$ when $r = r_{\max}$; $V = 0$ when $r = \infty$.

For Scheme B, the initial field has the following assumptions:

The temperature, geopotential height, wind and surface pressure fields have the same allocation as in Scheme A. The specific humidity field is derived by diagnostic analysis of the relative humidity and temperature fields. The initial relative humidity field is formed by superposing a high-humidity area on a horizontally homogeneous and typical-value-taken field. The center of the former coincides with that of vortex center of wind field. The horizontal distribution function $\mathbf{x}(r)$ takes

$$\mathbf{x}(r) = \mathbf{x}_k \exp\left[-12\left(\frac{r}{r_0}\right)^2\right] \quad (4)$$

where r carries the same meaning as above. It is known from the expression above that $\mathbf{x} = \mathbf{x}_k$ when $r = 0$; $\mathbf{x} = V_{\max}$ when $r = r_{\max}$; layers of \mathbf{x}_k take values differently and r_0 is a parameter in the expression in which the value is taken by $r_0 = \Delta\mathbf{q} \cdot a$, where a is the radius of the earth.

To reflect the asymmetric structure, the flow field of the entire TC flow field has to be determined before removing the symmetric parts of the flow field on each of the field. A deviation flow field is then obtained to highlight the asymmetry. The u and v values are first derived for each of the gridpoints to seek the location of gridpoints with the minimum velocity (i.e. $\sqrt{u^2 + v^2}$) for every layer. The point, O, can then be considered the center of TC, which is then originated to search along the x and y coordinates for four groups tangential wind speed at r distance from O. They are then averaged to obtain a symmetric flow field relative to the center O. A deviation field is then known by subtracting the field from the original one. Next is an analysis of the deviation field.

For the experiments above, all of the r_{\max} take $4r_0$ and the integration duration all take 48

h. Over the initial 6 h after the model run, no diabatic heating is added. After this point, a circular low pressure is formed at the bottom layer of the system due to the effect of adjustment. It can be viewed as a model TC or its fetus. The wind and pressure fields have by now reached an equilibrium state of quasi-gradient wind. The run then goes on with the inclusion of diabatic heating, except for the time of $d = 0$ when the process is always absent. The integration duration given in the paper includes the initial 6 h. Owing to the characteristics presented above for the initial field, the TC center is still some way off the boundary 48 h into the model integration, which justifies the view that the effect of boundary layer remains small during the period of integration.

3 NUMERICAL EXPERIMENT SCHEME

From some of the numerical experiments designed in Tab.1, we know that there are two kinds of experiments for Scheme A. The first is one that takes the Coriolis force as a constant, which is a mean over the domain integrated, i.e. those with “no” in the column of “-effect”. The second is one that takes the Coriolis force in the model in the form of $f = f_0 + \mathbf{b}y$, in which f_0 still uses the mean as presented above while \mathbf{b} has two cases in value taking: The first case is to take \mathbf{b} as a normal value, which corresponds to that in the center of the integrated domain (assuming $\mathbf{b} = 2\Omega \cos \mathbf{j}_0 / a$, with \mathbf{j}_0 being the latitude of integration center). It corresponds to the “yes” column in Tab.1. The second case is to double the normal value of \mathbf{b} to augment the effect, which fits the kind listed as “no” in Tab.1, i.e. the kind designated as “augmented” in the column of “-effect”. For Scheme B, the value of the Coriolis parameter f is taken as in usual numerical models if there is -effect but it assumes a constant if there is not.

Tab. 1 Content of numerical experiments

Experiment Serial No.	Schemes used	V_{\max}	d	Diabatic heating term	-effect
1	A	32	0	No	Yes
2	A	32	0	No	No
3	A	32	0	No	Augmented
4	A	12	5.78	Yes	Yes
5	A	12	5.78	Yes	No
6	A	12	5.78	Yes	Augmented
7	B	12	—	Yes	Yes
8	B	12	—	Yes	No

4 RESULTS OF NUMERICAL EXPERIMENTS

4.1 Exps.1, 2 & 3

In Exps. 1, 2 and 3, no diabatic heating is added, i.e. by taking $d = 0$. As the horizontal tangential wind speed takes relatively large values for model's initial field, it can be considered that the system evolves so that the structure becomes a tropical cyclone 6 h into integration. For the three experiments, the maximum wind speed evolves with integration time, as shown in the curves of Fig.1a, around the TC eye of the bottom layer of model TC (i.e. the lowest layer with $k=10$, same below). It is clear from the figure that the maximum wind is decreasing with integration time because there is frictional dissipation but no diabatic heating. At the middle layers, horizontal convergence and divergence are relatively small, which is similar to the evolution of real TC after it makes landfall.

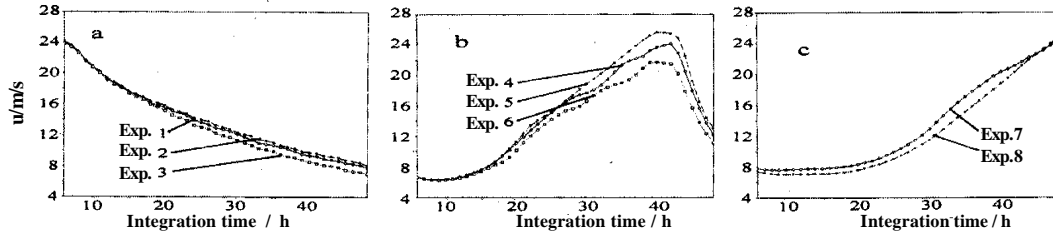


Fig.1 The evolution of maximum wind speed at the bottom layer with time. a. Exp.1, 2 & 3; b. Exp. 4, 5 & 6; c. Exp.7 & 8. Unit: m/s.

For Exp.1, the flow field of the middle layer (with $k=5$, same for all three experiments) is quasi-divergent due to the absence of diabatic heating. Fig.2 gives the corresponding deviation field of the middle layer flow field (asymmetric parts) 24 h and 48 h into the integration (Only portions of the circular zone are given and its center is the eye of TC, same below). It can be seen that the structure of the deviation field is such that cyclonic curvature is shown in the northwest of the model TC eye while anti-cyclonic curvature is displayed in the southeast. It is the so-called β -gyres. Subject to the condition, the model TC moves to the northwest. The experiment also shows that the model TC is free of the β -gyres structure in spite of asymmetric flow fields for both low and high layers (figure omitted). The structure appears only in the quasi-divergent-free middle layer.

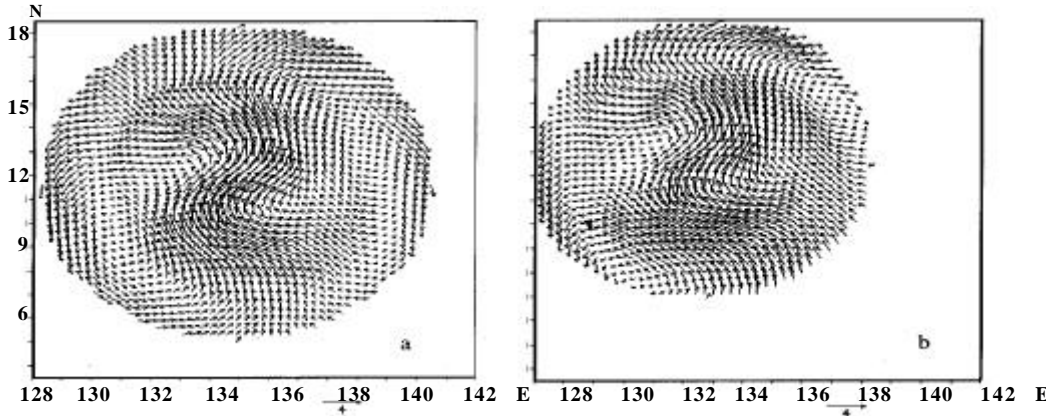


Fig.2 The deviation field of the middle-level stream field at the 24th h (a) and 48th h (b) in Exp.1. Unit : m/s.

For Exp.2, the asymmetry found in the model TC flow field has almost vanished and the β -gyres structure does not appear due to exclusion of the β -effect. The model TC remains stationary, too (figure omitted).

For Exp.3, the asymmetry of the flow field has increased and the β -gyres structure intensified due to increased β -effect. There is anti-cyclonic (cyclonic) curvature in the west (east) of the model TC eye, which is moving at greater speed towards northwest. Though with larger β -effect, the flow fields are still free of β -gyres structure at both low and high level flow fields (figure omitted).

4.2 Exps.4, 5 & 6

Scheme A is also used in Exps.4, 5 and 6 but taking into account the feedback effect of diabatic heating and the parameter β takes an homogeneous 5.78 for heating feedback adjustment. For the initial model field, V_{\max} takes an homogeneous 12 m/s. Six h into the integration without addition of diabatic heating, a fetus of model TC forms due to adaptation. The maximum near-surface wind speed has by now increased to about 9 m/s around the eye. For the evolution of the maximum wind speed at the model bottom layer of Exps.4, 5 and 6, see Fig.1b.

From Fig.1b, we know that the near-surface maximum wind speed has reached 20.1 m/s by the 31st h into the integration in Exp.4, suggesting the transformation of the fetus to a TC. Fig.3a

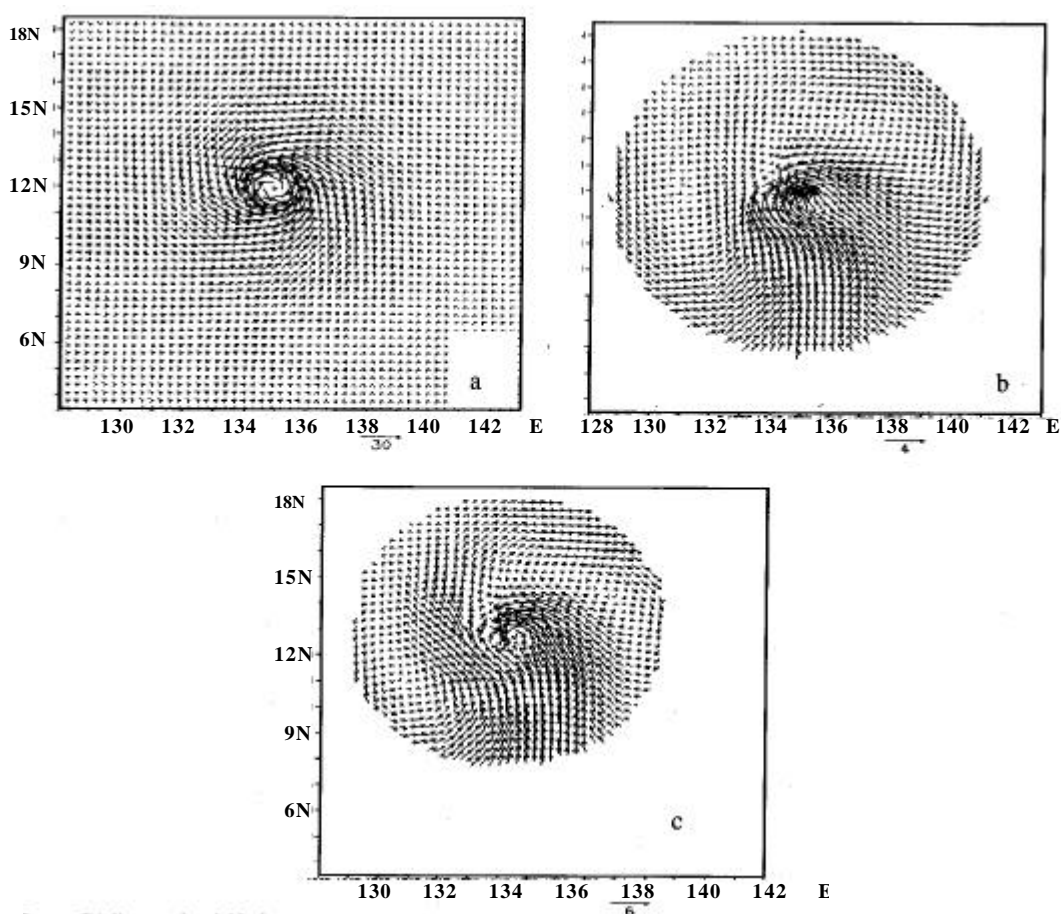


Fig.3 The bottom stream field (a) and the deviation field of the middle-level stream field (b) at the 36th hour in experiment 4 and the deviation field of the middle-level stream field at the 36th hour in experiment 6 (c). Unit is m/s.

gives the bottom-layer flow field 36 h into the integration when the maximum wind speed has increased to 23.9 m/s near the eye at the bottom layer of the model TC. Fig.3b gives the deviation of the middle-layer (i.e. $k=5$, applying to Exps.4, 5 & 6) flow field. It shows that the model TC is moving northwestward, which is obviously asymmetric in the flow field with anti-cyclonic (cyclonic) curvature in the northeast (southwest) of the eye, i.e. in the form of β -gyres structure. Southeasterly prevails between the cyclonic and anti-cyclonic curvature, namely the ventilation

flow. The experiment also tells us that the low-level flow field is fed with significant inflow while the high-level flow field with significant outflow. Like Exps.1 and 3, however, the flow fields for both low and high levels are free of the β -gyres structure (figure omitted).

Exp.5 doesn't take into the β -effect, either. From Fig.1b, we know that the maximum wind speed is already 20.2 m/s near the eye at the bottom layer when the model integrates for 29 h. It can be held that the fetus has then become a TC. Because of the lack of the β -effect, the flow field of the model TC remains symmetric, without the structure of β -gyres and the eye is also stationary (figure omitted).

For Exp.6, the β -effect is augmented artificially. From Fig.1b, the maximum wind speed has increased to 15.6 m/s near the eye at the bottom 24 h into the integration. Fig.3c gives the deviation of the middle-layer flow field 36 h into the integration. As the β -effect increases, the model TC moves northwest faster with more significant asymmetric flow field and well-defined β -gyres structure at the middle layer. In the northeast of the TC center is an anti-cyclonic vortex and the southwest a cyclonic vortex. The β -gyres structure is still absent from the low and high level flow fields (figure omitted).

4.3 Exps.7 & 8

For more realistic simulation of TC, Scheme B is used in Exps.7 and 8, which incorporates the specific humidity field. Exp.7 uses the β -gyres but Exp.8 doesn't. For the evolution of maximum wind speed with integration time near the eye of the bottom layer, see the curves in Fig.1c. It shows that it is already over 17 m/s 36 h into the integration when the TC fetus in both experiments has developed into TC.

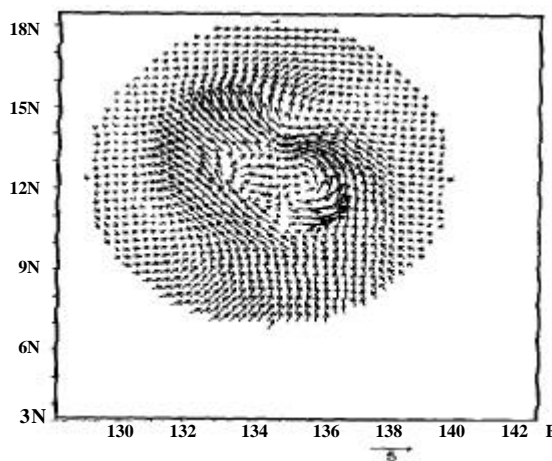


Fig.4 The deviation field of the middle-level stream field at the 48th hour in experiment 7. Unit: m/s.

Fig.4 gives the deviation of the middle-layer (with $k=6$, same in Exps.7 & 8) flow field 48 h into the integration in Exp.7. It shows clear a β -gyres structure, an anti-cyclonic vortex N-NE of the TC center but cyclonic curvature SE of it and powerful SE ventilation flow between them. It is noted that the β -gyres structure is absent in both low and high levels of the model TC during the experiments (figure omitted). As the parameterization of diabatic heating of Scheme A differs from that of Scheme B, the β -gyres structure is the most typical at the $k=6$ layer for Exps.7 and 8. For Scheme A, the $k=5$ layer has the most typical β -gyres structure.

For Exp.8, the lack of the β -effect leads to the absence of the β -gyres structure in the middle layer 48 h into the integration, with generally symmetric flow field and stationary eye of the TC (figure omitted).

5 QUANTITATIVE INTERPRETATION OF THE β -GYRES STRUCTURE

In a vortex equation that takes into account the β -effect approximation

$$\frac{dz}{dt} = -b v - f \left(\frac{\partial u}{\partial x} + \frac{\partial v}{\partial y} \right) \quad (5)$$

a pair of cyclonic, symmetric vortex is assumed for $t=0$, that is marked by significant convergence at the bottom level, and divergence at the upper level, of airflow. We then have at these levels that

$$\left| f \left(\frac{\partial u}{\partial x} + \frac{\partial v}{\partial y} \right) \right| \gg |b v| \quad (6)$$

where Eq.(5) can then be reduced to

$$\frac{dz}{dt} = -f \left(\frac{\partial u}{\partial x} + \frac{\partial v}{\partial y} \right) \quad (7)$$

As f is playing the role of a coefficient, the overall intensity of high-level anti-cyclone and bottom-level cyclone increases without changing the nature of the cyclone or anti-cyclone. For the middle layer, Eq.(5) can be simplified as below due to small convergence / divergence.

$$\frac{dz}{dt} \approx -b v \quad (8)$$

In the east of the vortex, $dz/dt < 0$ as $v > 0$ and $b > 0$, i.e. the vortex is less cyclonic and possibly turns into anti-cyclonic. On the other hand, the west of the vortex has $dz/dt > 0$ because $v < 0$, i.e. the vortex remains cyclonic with increased intensity. As a result, the -gyres structure will appear near the eye at the middle layer. It is noted that dz/dt is individual derivative so that elementary fluid parcels will rotate around the TC eye as the vorticity is increasing or decreasing. Such allocation will yield an anti-cyclonic center in its northeast but a cyclonic center in its southwest. It is then known that the -gyres result from the effect of the advection of geostrophic vorticity.

6 CONCLUDING REMARKS

a. When the geostrophic parameter is a constant, the -gyres are absent from the TC. Without the steering airflow, the TC eye does not rotate, either.

b. When the geostrophic parameter changes with the latitude, i.e. the -effect is present, the -gyres structure will appear with the increase of integration time in the middle layer of the TC.

c. With the -gyres in the middle layer of the TC, the eye will move northwest, to be consistent with the direction of the ventilation flow of the -gyres at the middle layer.

d. With the increase of the -effect, the TC becomes more asymmetric, the -gyres better-defined, the ventilation flow larger and the TC eye moves northwestward at faster speed.

e. The -gyres result from the effect of the advection of geostrophic vorticity.

In this paper, a simplified, ideal initial field is based to give results of numerical modeling and experiments. It is more necessary to do so for real cases of TC, which is just what we plan to do in future.

Acknowledgements: Mr. CAO Chao-xiong, who works at the Institute of Tropical and Marine Meteorology, CMA, Guangzhou, has translated the paper into English.

REFERENCES:

- [1] HOLLAND G J. Ambient interaction plus a Beta effect [J]. *Journal of Atmospheric Sciences*, 1983, **40**: 328-342.
- [2] FIORINO M , ELSBERRY R L. Some aspects of vortex structures related to tropical cyclone motion [J]. *Journal of Atmospheric Sciences*, 1989, **46**: 975-990.
- [3] CHEN Lian-shou. Status quo and development of research on and operational forecasting of tropical cyclone motion [A]. Proceedings of Symposium on Tropical Cyclones [C]. 1985. 6-30.
- [4] CHEN Lian-shou, XU Xiang-de, XIE Yi-yang, et al. The effect of tropical cyclone asymmetric thermodynamic structure on its unusual motion [J]. *Chinese Journal of Atmospheric Sciences*, 1997, **2**: 83-89.
- [5] XU Xiang-de, CHEN Lian-shou, XIE Yi-yang. The asymmetric and dynamic structure of the “-top” dipole and the “ventilation flow” of the target typhoon Flo during the TCM-90 field experiment [J]. *Acta Meteorologica Sinica*, 1996, **54**: 536-541.
- [6] LEE K L, ZHANG M. A numerical study on the orographic effect on the cold surge in southern China [A]. Climate environment & geophysical fluid dynamics, proceeding of the fourth international summer colloquium and international symposium for young scientists[C]. Beijing: China Meteorological Press, 1992. 123-128.